Rev. Roum. Sci. Techn.– Électrotechn. et Énerg.
Vol. **70**, *1*, pp. 63–68, Bucarest, 2025

EXPERIMENTAL DESIGN OF AN INTEGRAL BACKSTEPPING CONTROL FOR A SINGLE-PHASE SHUNT ACTIVE POWER FILTER

SABOUNI ELHADJ [1], BOUCHIBA BOUSMAHA[1], ABDELOUAHED TOUHAMI [1, 2], BESSADET IBTISSAM[1], BOUSSERHANE ISMAIL KHALIL[1]

Keywords: Power quality; Total harmonic distortion (THD); Active power filter; Backstepping control; Integral-backstepping controller.

This work has derived a cascaded two-loop nonlinear integral-backstepping-based control for single-phase shunt active power filter (SP-SAPF) to improve harmonic mitigation, reactive power compensation, and direct current link (DC-link) voltage regulation. Two loops of nonlinear controllers based on an Integral-backstepping strategy are developed, which are robust and stable in a wide range of output current, load variations, and DC-link voltage changes. First, the model of the SP-SAPF is exposed. Then, an integral backstepping control strategy is applied to the current loop to provide robustness to global control. Moreover, the compensation control system is then supported by another integral backstepping controller for DC-link voltage control to enhance DC-link loss compensation capability and generate the required active power, which the SAPF should take from the power supply. The active power filter (APF) control was designed and implemented using dSPACE 1103. The practical response of the developed controller is studied in some tests; it is shown that the proposed controller can eliminate harmonic components of the local load current with a fast dynamic response.

1. INTRODUCTION

With the increasing non-linear loads such as diode or thyristor front-end rectifiers, switching power supplies, and power electronic devices in power systems, power quality problems are deteriorating and attracting more attention. Active power filters (APFs) are widely applied in power systems to deal with distorted currents caused by non-linear loads [1–4]. (SP-SAPF) It is a good solution nowadays since it can solve harmonic current problems and compensate for the power factor. The SAPF has various advantages over passive ones since they don't need to be configured to a specific harmonic, but all harmonics are simultaneously compensated [5–7].

A direct control approach usually (SAPF) includes three control blocks [1,2,4]. The reference calculation unit performs online calculations of the local loads' reactive current and harmonic components. The current control unit applies appropriate switching signals so that the inverter output current follows the reference value. The DC-link voltage control unit adds an active element to the reference current according to the corresponding voltage error. In this case, despite power loss, the DC voltage of the inverter input can be kept constant at the desired reference value.

The grid current can be adjusted indirectly instead of controlling the inverter output current. The reference current of the grid can be formed according to grid alternative current (AC) voltage so that its amplitude is determined in a separate control loop based on the inverter DC side voltage error [1,2,4,8,9]. Considering that the SAPF is not capable of active power exchange with the power utility, if the DC-link voltage is regulated in the desired value and the grid current becomes pure sinusoidal, it can be concluded that the local load harmonic and reactive components are compensated completely. In the indirect control method, reference current calculation and DC-link voltage control units are combined, significantly reducing required calculations in SAPFs; hence, system dynamic response can be improved considerably. In the indirect control approach, SAPF includes only two control loops [10–15]. First, the voltage outer loop determines the grid reference current based on the DC-link voltage error for the inner loop, and second, the inner current loop controls the inverter output current using a pulse-width modulation (PWM) switching scheme.

In this paper, an integral backstepping controller design for DC-link voltage and compensation current control of SP-SAPF has been investigated and derived, which yields good performance under load increase/decrease. The rest of the paper is organized as follows: the SAPF model is described in section 2, the control design of integral backstepping control for SAPF is developed and presented in section 3, the experimental result using dSPACE 1103 of different studied cases is defined in section 4, and the conclusion is drawn in section 5.

2. SYSTEM MODELLING

The SP-APF under study has the structure of Fig.1 considering the H-bridge inverter [6–8, 16–18]. It is assumed that the inverter is switched using the bipolar PWM technique. From the AC side, the APF is connected to the primary AC voltage source through the filtering inductor L_f in parallel with a nonlinear load. The role of the SAPF is to produce reactive and harmonic components to compensate undesirable current harmonics produced by the nonlinear load doing so; the filter-load association behaves as a pure resistive load, which amounts to making the fundamental component of load current in phase with the main AC voltage [8,10].

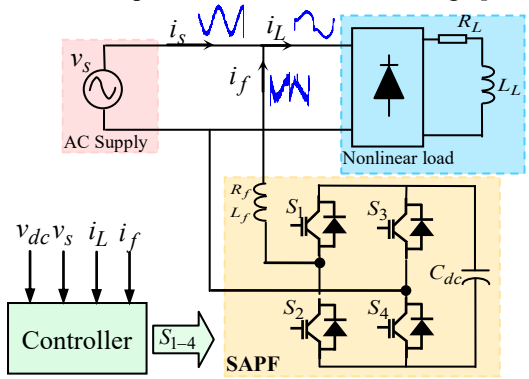

Fig. 1 – Principle scheme of single-phase shunt active power filter SAPF.

[1] Laboratoire des énergies renouvelables et les réseaux intelligents, Université Tahri Mohamed of Bechar, Algeria.
E-mails : {sabouni.elhadj, bouchiba.bousmaha, ismail.bousserhane}@univ-bechar.dz, bessadet.ibtissam@gmail.com,
[2] Department of Electrical Systems Engineering, University M'Hamed Bougara of Boumerdes, Algeria.
E-mail: a.touhami@univ-boumerdes.dz

DOI: 10.59277/RRST-EE.2023.1.11

To study the SAPF's behavior with the electrical network, a mathematical model of the whole network must first be established, and an active power filter and nonlinear load must be shunted.

Applying the usual Kirchhoff's laws to the SP-SAPF, one quickly gets [5–7, 15–21]

$$\begin{cases} L_f \frac{\mathrm{d}i_f}{\mathrm{d}t} = v_s - R_f i_f - v_{AB}, \\ C_{dc} \frac{\mathrm{d}v_{dc}}{\mathrm{d}t} = i_{dc}, \end{cases} \quad (1)$$

where L_f denotes the filter inductance, R_f the filter resistor, C_{dc} DC side capacitor, v_s the power supply voltage, v_{AB} the inverter AC voltage, v_{dc} the DC-link voltage, and the DC-side current.

The inverter equations

$$\begin{cases} v_{AB} = \mu \cdot v_{dc}, \\ i_{dc} = \mu \cdot i_f, \end{cases} \quad (2)$$

where the switching function μ of the inverter is defined by:

$$\begin{cases} 1 & \text{if } (S_1,S_4) \text{ are ON; } (S_2,S_3) \text{ are ON,} \\ -1 & \text{if } (S_1,S_4) \text{ are ON; } (S_2,S_3) \text{ are ON.} \end{cases} \quad (3)$$

Combining (1) and (2), one obtains the instantaneous model of the whole system [15, 16]

$$\begin{cases} \frac{\mathrm{d}i_f}{\mathrm{d}t} = \frac{1}{L_f}\left(v_s - R_f i_f - \mu \cdot v_{dc}\right), \\ \frac{\mathrm{d}v_{dc}}{\mathrm{d}t} = \frac{1}{C_{dc}} \mu \cdot i_f. \end{cases} \quad (4)$$

3. CONTROL DESIGN

The synthesis of the controller is based on two steps. First, an outer loop is constructed to achieve voltage regulation on the DC-link of the SAPF. In the second step, an inner current loop is designed to deal with the current harmonic elimination and the power compensation problem.

3.1 REFERENCE CURRENT IDENTIFICATION FOR HARMONIC CURRENT COMPENSATION

In literature, several methods and techniques have been proposed to generate the reference current of compensation for the SAPF [4, 22–26]. This section discusses the reference current identification for harmonic current mitigation based on active and reactive instantaneous power techniques [26-29]. This technique measures the power supply voltage v_s and load current i_L and transforms it into a pseudo-two-phase frame. The two phases are transformed to apply the generalized single-phase instantaneous *p-q* theory. Based on the instantaneous $\pi/2$ lead of the grid voltage v_s and load current i_L, it's considered a fictitious pseudo-two-phase system [26]. So, the overall system can be expressed in α-β coordinates. The grid voltage and load current are considered as the fictitious voltage and current of the α-axis ($v_{s\alpha} = v_s$, $i_{L\alpha} = i_L$). Subsequently, $v_{s\alpha}$ it produces source voltage and load current on the β-axis ($v_{s\beta}$, $i_{L\beta}$). Therefore, the single-phase source voltage and load current representation in αβ-axes is given by [26,29]:

$$\begin{bmatrix} v_{s\alpha} \\ v_{s\beta} \end{bmatrix} = \begin{bmatrix} v_s \\ v_s(\pi/2) \end{bmatrix}, \quad (5)$$

$$\begin{bmatrix} i_{L\alpha} \\ i_{L\beta} \end{bmatrix} = \begin{bmatrix} i_L \\ i_L(\pi/2) \end{bmatrix}. \quad (6)$$

The instantaneous active and reactive power, *p* and *q*, are expressed as [26, 29]:

$$\begin{bmatrix} p \\ q \end{bmatrix} = \begin{bmatrix} \tilde{p}+\bar{p} \\ \tilde{q}+\bar{q} \end{bmatrix} = \begin{bmatrix} v_{s\alpha} & v_{s\beta} \\ -v_{s\beta} & v_{s\alpha} \end{bmatrix} \begin{bmatrix} i_{L\alpha} \\ i_{L\beta} \end{bmatrix}, \quad (7)$$

where $\bar{p}$ and $\bar{q}$ denote the DC components, which correspond to the fundamental active and reactive power, whereas $\tilde{p}$ and $\tilde{q}$ represent the AC components responsible for harmonic power. So, the compensation current reference for harmonic mitigation can be extracted by [26,29]

$$\begin{bmatrix} i_{f\alpha} \\ i_{f\beta} \end{bmatrix} = \frac{1}{v_{s\alpha}^2 + v_{s\beta}^2} \begin{bmatrix} v_{s\alpha} & -v_{s\beta} \\ v_{s\beta} & v_{s\alpha} \end{bmatrix} \begin{bmatrix} -\tilde{p}+\bar{p}_{dc} \\ -q \end{bmatrix}. \quad (8)$$

The term $\tilde{p}$ can be calculated from the active power *p* using a high-pass filter. The block diagram, which generates the reference current of compensation for the shunt active power filter based on the instantaneous *p-q* power theory, is illustrated in Fig. 2.

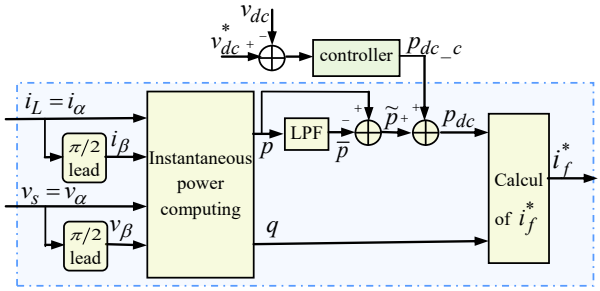

Fig. 2 – Block diagram for generating the reference current of compensation.

3.2. OUTER-LOOP CONTROLLER DESIGN

This loop adjusts the grid reference current i_s^* and determines the filter reference current i_f^* so that the DC-link voltage equals its reference value v_{dc}^*.

Define the first error variable as:

$$e = v_{dc}^* - v_{dc}, \quad (9)$$

where '*' denotes the reference values.

We introduce then a new tracking error given as:

$$e_1 = k_1 e + k_2 \int e \cdot \mathrm{d}t, \quad (10)$$

with k_1 and k_2 are positive constants

Compute the derivative of e_1

$$\begin{aligned} \dot{e}_1 &= k_1 \dot{e} + k_2 e \\ &= k_1 \left(\dot{v}_{dc}^* - \dot{v}_{dc}\right) + k_2 e. \end{aligned} \quad (11)$$

Considering the equation system (1), the expression of $\dot{e}_1$ can be written as:

$$\dot{e}_1 = k_1 \dot{v}_{dc}^* - k_1 \frac{1}{C_{dc}} \frac{P_{dc}}{v_{dc}} + k_2 e, \quad (12)$$

with

$$i_{dc} = \frac{P_{dc}}{v_{dc}}, \quad (13)$$

where P_{dc} represents a direct component of the power.

Lyapunov function V_1 is chosen as

$$V_1 = \frac{1}{2} e_1^2 \quad (14)$$

We differentiate (14) to get:

$$\dot{V}_1 = e_1 \cdot \dot{e}_1, \quad (15)$$

then substitute eq. (11) into (15) to obtain

$$\begin{aligned} \dot{V}_1 &= e_1 \left(k_1 \dot{v}_{dc}^* - k_1 \frac{1}{C_{dc}} \frac{P_{dc}}{v_{dc}} + k_2 e\right) \\ &= -C \cdot e_1^2 + e_1 \left(k_1 \cdot \dot{v}_{dc}^* - \frac{k_1}{C_{dc}} \frac{P_{dc}}{v_{dc}} + k_2 \cdot e\right), \end{aligned} \quad (16)$$

where C is a positive design constant. The tracking DC voltage objectives are achieved if the control law is designed as

$$P_{dc}=\frac{C_{dc}v_{dc}}{k_1}\left(C\cdot e_1+k_1\dot{v}_{dc}^{*}+k_2\cdot e\right). \quad (17)$$

Substituting (17) into (16) yields

$$\dot{V}_1=-C\cdot e_1^2. \quad (18)$$

Thus, the virtual control is asymptotically stable.

3.3. INNER-LOOP CONTROLLER DESIGN

This controller adjusts the converter switching signal to regulate the filter output current in its corresponding reference value $i_f^{*}=i_L-i_s^{*}$. SAPF will supply the reactive and harmonic components of load current in this case. Considering the non-linear nature of the SAPF, in this paper, an integral backstepping controller has been employed for the system's inner loop. System model parameters are uncertain. The integral backstepping controller for single-phase SAPF is designed as follows

$$e_2=i_f^{*}-i_f, \quad (19)$$

where i_f^{*} represents the reference compensating current.

We define a new tracking error as follows:

$$z=c_1\cdot e_2+c_1\int e_2\cdot \mathrm{d}t, \quad (20)$$

with c_1, c_2 are positive constants.

It is possible to write the derivative of the first error variable as

$$\begin{aligned}\dot{z}&=c_1\cdot\dot{e}_2+c_2\cdot e_2\\&=c_1\left(\dot{i}_f^{*}-\dot{i}_f\right)+c_2\cdot e_2.\end{aligned} \quad (21)$$

Taking into account the model of the SAPF, we can write:

$$\dot{z}=c_1\cdot\left(\dot{i}_f^{*}-\frac{1}{L_f}\left(v_s-R_f i_f-\mu\cdot v_{dc}\right)\right)+c_2e_2. \quad (22)$$

Then, the Lyapunov function V_2 can be considered as

$$V_2=\frac{1}{2}z^2. \quad (23)$$

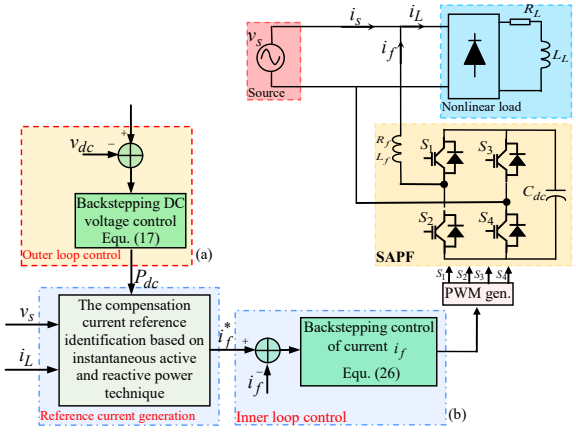

Fig. 3 – Block diagram of the proposed controller for single-phase APF (a) Outer loop controller design, (b) Inner loop control

We differentiate the Lyapunov function V_2 in (23) and substitute the error dynamic equation to get

$$\begin{aligned}\dot{V}_2&=z\cdot\dot{z}\\&=z\left(c_1\dot{i}_f^{*}-\frac{c_1}{L_f}v_s+\frac{c_1}{L_f}R_f i_f+\frac{c_1}{L_f}\mu v_{dc}+c_2e_2\right).\end{aligned} \quad (24)$$

Then, we can write

$$\dot{V}_2=-Kz^2+z\left(c_1\dot{i}_f^{*}-\frac{c_1}{L_f}\left(v_s+R_f i_f+\mu v_{dc}\right)+c_2e_2\right). \quad (25)$$

If the control action μ is selected as follows:

$$\mu=\frac{L_f}{c_1v_{dc}}\left(K\,z+c_1\dot{i}_f^{*}+\frac{c_1}{L_f}v_s-\frac{c_1R_f}{L_f}i_f+c_2e_2\right), \quad (26)$$

where K is a positive design constant. Thus, the eq. (25) becomes

$$\dot{V}_2=-K\cdot z^2\le 0. \quad (27)$$

Thus, the control signal is asymptotically stable. Figure 3 illustrates the principle scheme of the integral backstepping control for SP-SAPF.

4. EXPERIMENTAL RESULTS

The effectiveness of the SP-SAPF based on the proposed integral backstepping controller for current harmonic mitigation has been experimentally verified using dSPACE 1103 R&D board and Control Desk experiment software. Circuit topology and the overall experimental setup are illustrated in Fig. 4. As shown in Fig. 4, the experimental platform consists of the nonlinear load, which is composed of a full-bridge diode rectifier with RL load, a full-bridge inverter IGBT modules (SK40GB 123 Semikron) employed as a primary circuit of the SP-SAPF. The compensation and load currents are measured using Hall-effect LEM current sensors, whereas two voltage sensors measure the source and DC link voltages. The specific nominal circuit parameters of the SP-SAPF prototype are $v_s^{rms}=41$ V, $R_L=100\ \Omega$, $L_L=35$ mH, $R_f=0.25\ \Omega$, $L_f=9$ mH, $v_{DC}=79.8$ V, $C_{DC}=2200\times10^{-6}$ F.

To increase the load value, a switch-insulated gate bipolar transistor (IGBT) is controlled via the digital output of dSPACE-1103 to short-circuit an additive resistor, which is connected in series with the main RL load. At the starting time, the IGBT is in an OFF state, and at a specified time (6.067 s for the scenario test), the switch state is converted to "ON'' by sending a stop signal to suppress the additive resistance.

In this paper, an experimental test platform has been done for one test operating conditions scenario to verify the effectiveness of the proposed method analysis. The test scenario consists of a step change in DC-link voltage value from 0 V to 78.75 V (which is equal to 1.8 v_s^{rms}, see [4,8] for more detail). The SP-SAPF circuit is started with a constant load, and then, the additive resistor is removed (short-circuited) using an IGBT switch at $t=6.054$ s. The additive resistor is then added to the main load at $t=8.05$s when the IGBT state is converted to OPEN by sending a 0 V from the digital output of dSpace-1103.

The different experimental waveform results are shown in Fig. 5-15. The load current waveform is shown in Fig. 5. It's highly distorted and has rich harmonics due to the nonlinear load characteristic. Figure 6 shows the source current waveform without and with active power filter compensation. From this figure, we can observe that the source current has a sinusoidal form. The waveforms presented in Fig. 6,b and 6,c show that the value of the source current is increased and decreased against the rising or decreasing load resistance value. The experimental results show that the integral backstepping controller forces the generated filter current to track its reference correctly when the value of the nonlinear load changes (see Fig. 7).

Furthermore, it is clearly shown that when the

measurement is started, the source current is equal to the load current before the SAPF activation ($t_{act} = 1.39$ s), its form becomes sinusoidal when the compensating current is injected due to the SAPF activation, as presented in Fig. 8.

Moreover, the DC-link voltage is kept using the proposed controller around its desired value with minimal rising time, small undershoots, and overshot against load increasing/decreasing (see Fig. 9).

Figure 10 illustrates a comparison result between the classical PI controller and the proposed integral backstepping controller. The proposed nonlinear controller provides better control performances than the PI control. Figures 11 and 12 illustrate the harmonic spectrum of the load and the source currents, respectively. From Fig. 11, it can be observed that the load current presents a high value of around 23 %. Moreover, it's seen in Fig. 12 that the total harmonic distortion (THD) of the source current was reduced considerably to 4.2 % by compensation, which is below the requirement of the IEEE 519 standards (5 %).

Figure 13 depicts the grid current and the source voltage. As can be easily shown from this figure, the grid current is in the same phase as the source voltage, which confirms that the power factor under operation conditions is equal to 1. From the results, the proposed controller for SP-SAPF current harmonic mitigation shows good performance and is effective against increasing and decreasing load.

For further demonstration of the effectiveness of the proposed integral backstepping controller, a comparison with other related works found in the literature can be shown in Table 1.

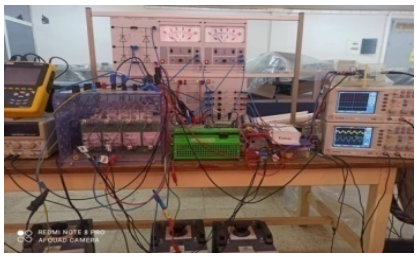

(a)

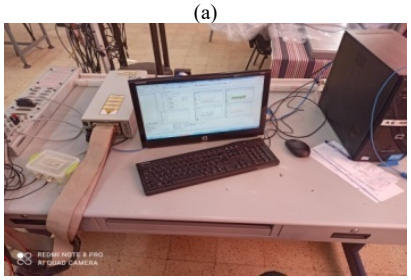

(b)

Fig. 4 – Experimental setup of the single-phase APF (a) Single phase APF (b) PC and dSPACE 1103.

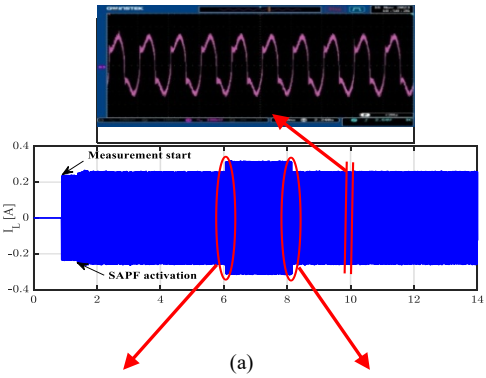

(a)

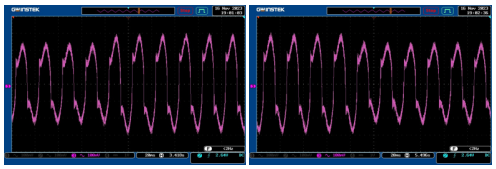

(b) (c)

Fig. 5 – Load current i_L: (a) Load current waveform (b) i_L during load increasing (c) i_L during load decreasing.

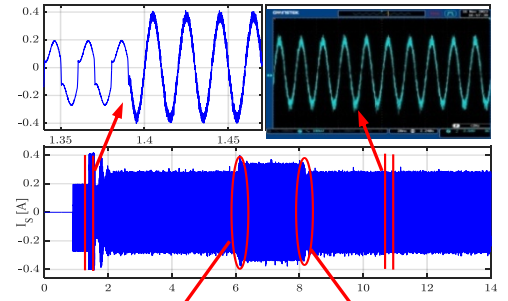

(a)

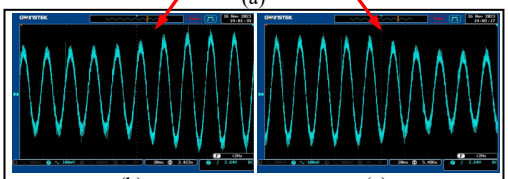

(b) (c)

Fig. 6 –Source current i_s: (a) source current waveform (b) i_s during load increasing (c) i_s during load decreasing.

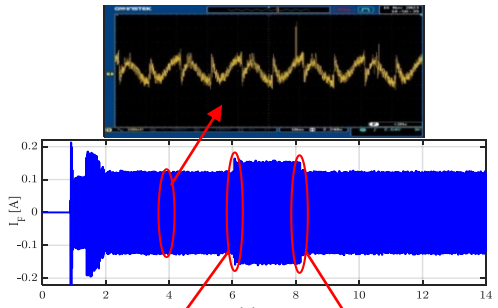

(a)

(b) (c)

Fig. 7 – Compensation current, i_f: (a) Compensation current waveform (b) i_f during load increasing (c) i_f during load decreasing.

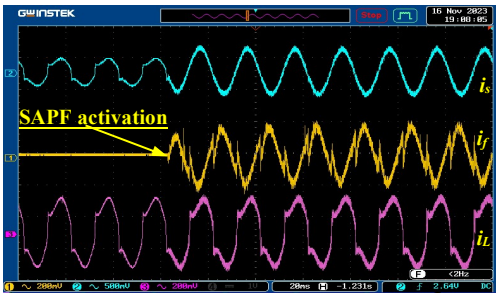

Fig. 8 – Source, compensation, and load currents waveforms.

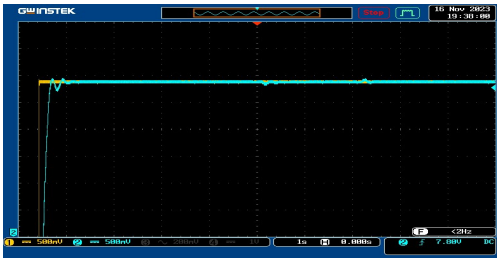

(b)

Fig. 9 – DC link voltage v_{dc} waveform.

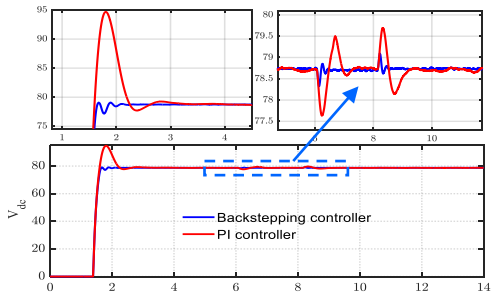

Fig. 10 – Comparison of DC-link voltage v_{DC} responses between PI controller and integral backstepping control.

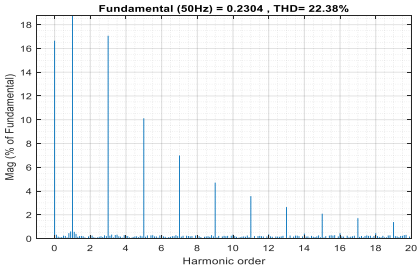

Fig. 11 – Harmonic spectrum of load current i_L.

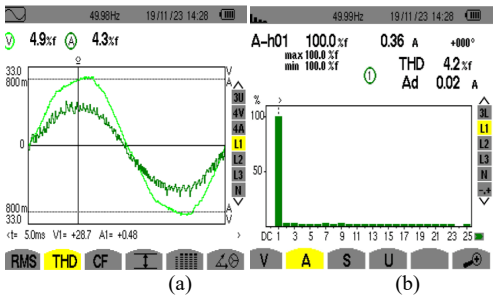

(a) (b)

Fig. 12 – Source voltage and current waveforms and their THD
(a) Harmonic distortion THD of v_s and i_s (b) harmonic spectrum of the i_s.

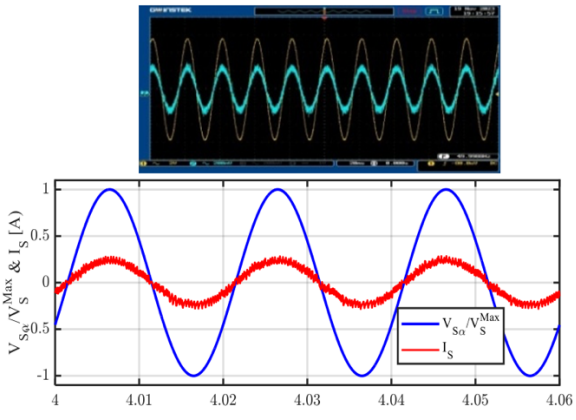

Fig. 13 – The source voltage v_s and source current i_s waveforms.

Table 1

Comparison with related works

	[30]	Proposed
Outer loop controller	PID controller	Integral backstepping
Inner loop controller	Backstepping	Integral backstepping
Compensating current identification method	Indirect current extraction method	Instantaneous active/reactive method
Experimental setup	No	Yes
v_{dc} response rising-time	0.3 s	0.26 s
Source current THD	Not mentioned	4.2 %

5. CONCLUSION

This paper proposes Nonlinear SP-SAPF control using a backstepping controller to enhance current harmonic and reactive power compensation in the presence of nonlinear and uncertain loads and tight voltage regulation at the inverter output capacitor. The accuracy and effectiveness of the designed nonlinear controller for the SP-SAPF are successfully verified by experimental setup using dSPACE 1103, considering different steady and transient state tests.

The results show that the proposed controller is practical, robust, and stable against load increase/decrease and uncertainty. So, the control objectives have been achieved in terms of compensation, his reference and regulation will follow the current, and the voltage is stabilized at its reference value, ensuring a stable system situation for an extensive range of operation conditions.

Therefore, the single-phase shunt active power filters with the proposed integral backstepping controller can provide good control performances, high accuracy, and convergence with less complexity and processor computing compared to another nonlinear controller.

CREDIT AUTHORSHIP CONTRIBUTION STATEMENT

Sabouni Elhadj: methodology, development, software simulation, experimental validation, writing & review, analysis
Abdelouahed Touhami: methodology, development, software simulation, writing & review, analysis.
Bessadet Ibtissam: methodology, development, software simulation, writing & review of experimental validation
Bouchiba Bousmaha: supervision, development, writing & review, experimental validation, analysis
Bousserhane Ismail Khalil: supervision, development, writing & review, experimental validation, analysis

Received on 30 April 2024

REFERENCES

1. B. Singh, A. Chandra, K. Al-Haddad, *Power quality problems and mitigation techniques*, John Wiley & Sons Ltd. (2014).
2. S. Perera, S. Elphick, *Applied power quality analysis, modelling, design and implementation of power quality monitoring Systems*, Elsevier (2023).
3. P.S. Revuelta, S. P. Litrán, J.P. Thomas, *Active power line conditioners design, simulation and implementation*, Academic Press (2016).
4. S. Biricik, O.C. Ozerdem, S. Redif, M.S. Dincer, *New hybrid active power filter for harmonic current suppression and reactive power compensation*, International Journal of Electronics, **103**, *8*, pp. 1397–1414 (2016).
5. S. Echalih et al., *A cascaded controller for a grid-tied photovoltaic system with three-phase half-bridge interleaved buck shunt active power Filter: hybrid control strategy and fuzzy logic approach*, IEEE Journal on Emerging and Selected Topics in Circuits and Systems, **12**, *1*, pp. 320–330 (2022)
6. S. Echalih, A. Abouloifa, I. Lachkar, Z. Hekss, A. el Aroudi, F. Giri, *Nonlinear control design and stability analysis of single-phase half-bridge interleaved buck shunt active power Filter*, IEEE

Transactions on Circuits and Systems I, **69**, *5*, pp. 2117–2128 (2022).
7. L. Zhang, J. Fei, *Intelligent complementary terminal sliding mode using multiloop neural network for active power filter*, Ieee Transactions on Power Electronics, **38**, *8*, pp. 9367–9383 (2023).
8. S. Biricik, *Grid voltage sensorless single-phase half-bridge active filter and DC bus voltage regulation*, Electric Power Components, and Systems, **19**, pp. 2131–2140 (2017).
9. F. Bagheri, S. Biricik, H. Komurcugil, *A DC side sensorless single-phase shunt active power filter with a second order sliding mode control and unbalance loads*, *14th Power Electronics, Drive Systems, and Technologies Conference (PEDSTC)*, Iran, pp. 1–5 (2023).
10. S. Biricik, S. Redif, K. Shafiuzzaman, B. Malabika, *Improved harmonic suppression efficiency of single-phase APFs in distorted distribution systems*, International Journal of Electronics, **103**, *2*, pp. 232–246 (2016).
11. A. Krama, L. Zellouma, A. Benaissa, B. Rabhi, M. Bouzidi, M.F. Benkhoris, *Design and experimental investigation of predictive direct power control of three-phase shunt active filter with space vector modulation using anti-windup PI controller optimized by PSO*. Arab J. Sci. Eng., **44**, pp. 6741–6755 (2019).
12. O. Aissa, O. Gherouat, B. Babes, F. Albalawi, A. Alqurashi, S.S.M. Ghoneim, *Experimental validation of advanced SP-SAF based on intelligent controllers for power quality enhancement*, Energy Reports, **8**, pp. 3018–3029 (2022).
13. A.M. Dumitrescu, G. Griva, R. Bojoi, V. Bostan, R. Măgureanu, *Current controllers design using naslin polynomial method for active power filters*, Rev. Roum. Sci. Techn. – Électrotechn. Et Énerg., **54**, *1*, pp. 115–124 (2009).
14. A. Hamdaoui, A. Semmah, A. Masssoum, P. Wira, A. Ayad, A. Meroufel, *Elaboration of a fuzzy switching table for the control of an active power filter*, Rev. Roum. Sci. Techn. – Électrotechn. Et Énerg., **58,** 4, pp. 405–414 (2013).
15. L. Deng, J. Fei, C. Cai, *Global fast terminal sliding mode control for an active power filter based on a backstepping design*, Rev. Roum. Sci. Techn. – Électrotechn. Et Énerg., **61**, 3, pp. 293–298 (2016).
16. Q. Pan, Y. Zhou, J. Fei, *Feature selection fuzzy neural network super-twisting harmonic control*, Mathematics **11**, pp. 1495 (2023).
17. J. Fei, L. Zhang, J. Zhuo, Y. Fang, *Wavelet fuzzy neural super-twisting Sliding mode control of an active power filter*, IEEE Transactions on Fuzzy Systems, **31**, *11*, pp. 4051–4063 (2023).
18. J. Fei, Z. Wang, Y. Fang, *Self-Evolving recurrent Chebyshev fuzzy neural sliding mode control for active power filter*, IEEE Trans. on Industrial Informatics, **19**, *3*, pp. 2729–2739 (2023).
19. Q. Pan, J. Fei, Y. Xue, *Adaptive intelligent super-twisting Control of dynamic system*, IEEE Access, **10**, pp. 42396–42403 (2022).
20. M. Salimi, J. Soltani, A. Zakipour, *Experimental design of the adaptive backstepping control technique for single-phase shunt active power filters*. Iet Power Electronics, **10**, pp. 911–918 (2017).
21. S. Hou, J. Fei, Y. Chu, C. Chen, *Experimental investigation of adaptive fuzzy global sliding mode control of single-phase shunt active power filters*, IEEE Access, **7**, pp. 64442–64449 (2019).
22. M. Fallah, J. Modarresi, A. Ajami, M.B. Tavakoli, *improvement of Indirect Harmonic Compensation Method Using Online Discrete Wavelet Transform*, Journal of Circuits, Systems and Computers. **25**, *04*, pp. 1650019 (20 pages) (2015).
23. M. Fallah, J. Modarresi, H.M. Kojabadi, L. Chang, J.M. Guerrero, *A modified indirect extraction method for a single-phase shunt active power filter with smaller DC-link capacitor size*, Sustainable Energy Technologies and Assessments, **45**, pp. 101039 (15 pages), pp. 1-15 (2021).
24. M.-S. Karbasforooshan, M. Monfared, M. Dogruel, *Indirect control of single-phase active power filters using harmonic control arrays*, Conference on Electrical Power Distribution Networks Conference (EPDC), Semnan, Iran, pp. 143–148 (2017).
25 J. Miret, M. Castilla, J. Matas, J.M. Guerrero, J.C. Vasquez, *Selective harmonic-compensation control for single-phase active power filter with high harmonic rejection*, IEEE Trans. on Industrial Electronics, **56**, *8*, pp. 3117–3127 (2009).
26. V. Khadkikar, A. Chandra, B.N. Singh, *Generalized single-phase p-q theory for active power filtering: simulation and DSP-based experimental investigation*, IET Power Electronics, **2**, *1*, p. 67–78 (2009).
27. A. Chebabhi, M.K. Fellah, M.F. Benkhoris, *3D space vector modulation control of four-leg shunt active power filter using pq0 theory*, Rev. Roum. Sci. Techn. – Électrotechn. Et Énerg., **60**, *2*, pp.185–194 (2015).
28. S. Chennai, *Three-level neutral point clamped shunt active power filter performances using intelligent controllers*, Rev. Roum. Sci. Techn. – Électrotechn. Et Énerg., **59**, *3*, pp. 303–313 (2014).
29. V.N. Jayasankar, U. Vinatha, *Backstepping controller with dual self-tuning filter for single-phase shunt active power filters under distorted grid voltage condition,* IEEE Transactions on Industry Applications, **56**, 6, pp. 7176–7184 (2020).
30. A. Elallali, A. Abouloifa, I. Lachkar, C. Taghzaoui, A. Hamdoun, *Backstepping control for shunt active power filters, controller design, and average performance analysis*, International Conference on Automation, Control Engineering and Computer Science (ACECS), France (2017).